Conductivity Variation Induced by Solvent Swelling of an Elastomer–Carbon Black–Graphite Composite

ALFREDO MARQUEZ, JORGE URIBE, RICARDO CRUZ

Centro de Investigación Científica de Yucatán, Km. 7 ant. carr. a Progreso, A.P. 87, Cordemex, C.P. 97310, Mérida, Yucatán, México

Received 17 November 1995; accepted 2 June 1997

ABSTRACT: The behavior of a polybutadiene–carbon black composite entering into contact with organic solvents and gasoline was investigated. The composite used has a conductivity of $3.0 \pm 0.1\ \Omega^{-1}\ cm^{-1}$. However, if it comes into contact with organic solvents (gasoline, for instance) the matrix absorbs them and consequently swells. This swelling causes the separation of the carbon particles and the concomitant diminution of the composite conductivity. During the tests performed, the resistivity of the composite grows exponentially with the exposure time to solvents. Typically, the material samples show a reduction of approximately 30% of its initial conductivity after only 1.5 min of exposure to solvents. Also, it was observed that the rate at which the conductivity decreases is related to the chemical nature of the solvent used in the test. To model the drop on composite conductivity induced by solvent swelling we use an effective media percolation approach. This approach was adapted to the needs of our experiments by modifying the definition of one of its main parameters (the critical volume of the low-conductivity fraction). The experimental data were successfully described by this model. Finally, the test performed shows that this composite is a very promising material that can be employed, for example, in various security and control devices to warning of accidental organic solvent or hydrocarbon leaks in pipelines or containers of chemical industries and refineries. J Appl Polym Sci **66:** 2221–2232, 1997

Key words: electric; polymeric; composite; swelling; solvents

INTRODUCTION

Little attention has been paid in the literature to the effect of organic solvents on the electrical properties of polymeric conductive composites. For example, after an extensive bibliographic search,[1–101] we found just two scientific papers,[1,2] some patents,[3–6] and one thesis[85] on the topic. Nevertheless, it is important to stress that using polymer composites, especially the elastomeric ones, it is possible to design and produce sensors capable of detecting leakages of organic solvents or gasolines. These sensors can be employed in various security and control devices for pipelines or containers in industrial plants, refineries, or gas stations.[3–6] Indeed, it is possible to design an electric conductive composite that would be sensitive to organic solvents.

Polymers and organic solvents are usually excellent electrical insulators; however, it is possible to make up polymer composites with a relatively good electrical conductivity by adding conductive particles to the polymer at concentrations above a threshold called "the electrical percolation concentration." On the other hand, for each organic solvent used in the industry there is at least one

Correspondence to: A. Marquez.
Contract grant sponsor: CONACyT; contract grant number: G500–55/95.

Journal of Applied Polymer Science, Vol. 66, 2221–2232 (1997)
 CCC 0021-8995/97/122221-12

polymer capable of absorbing it by a dissolution or swelling process. Hence, by choosing a polymer with high affinity for a determinate solvent, it is possible, by filling it with electrical conductive particles, to make up a composite that changes its electrical properties when it comes into contact with this solvent. This is possible because the swelling of the matrix by the solvent causes the separation of the conductive particles into the composite, producing a decrease of its electrical conductivity. This effect is produced, in a reversible way in several composites, especially in those filled with carbon black.[1]

In our laboratory we have developed an electrical conductive composite that is sensible to the presence of organic solvents and gasolines. This composite is constituted of an elastomeric matrix highly filled with two types of carbon particles: carbon-black and graphite. The carbon black imparts the main electrical characteristics of the composite, but also causes an important increase of its viscosity. This fact avoids the processing of composite by fast molding methods such as extrusion or injection. Therefore, to diminish the composite viscosity, graphite was added as a lubricant during the shaping processes. The resulting composite has an acceptable conductivity ($\sigma \sim 3\ \Omega^{-1}$-$cm^{-1}$), and a viscosity of 3.98×10^4 Pa s (measured at 190°C and a strain rate of 10 s^{-1}).

On the other hand, it is important to indicate that several theories have been developed to describe the properties of the conductive polymeric composites with an aleatory distribution of the conducting particles. Among such theories the more important ones are: the percolation theory, which describes macroscopically the electrical flow through a medium haphazardly distributed[7–78]; and the tunnel effect theory, which describes microscopically the passage of electrons through a thin potential barrier, for example, the polymer layers that cover the conducting particles in a polymer composite.[7,79–83]

The percolation theory describes the formation of a continuous path of conductive particles where the electrons can flow. To form this path it is necessary to reach a certain concentration of conductive particles, such concentration is called "electrical percolation concentration." At this concentration the particles come into electrical contact and generate a continuous mesh. There are several percolation models such as statistical, geometrical, thermodynamical, etc.[87] However, the effective media theory[8] may be the more general one. This theory was successfully used to predict the effective, or large volume average, of the electrical and thermal conductivities, dielectric constant, gaseous diffusion, and magnetic permeability of composites. In the present work we use this last model to describe the variations on the composite conductivity induced by solvent swelling.

Table I Matrix Characteristics

Industrial Grade	S200
Structure	Branched
Microstructure (w/w %):	
Cis 1,4	44.0
Trans 1,4	47.0
Vynil 1,2	9.0
Stabilizers (w/w %)	0.400
M_n	344.600
M_w	494.900
Density at 25°C (g/cm^3)	1.01 ± 0.01
Degrading temperature (°C)	220.0 ± 5.0
Melt Index (g/10 min)	0.961 ± 0.01 (190°C)

EXPERIMENTAL

Materials and Processing of the Composite

The matrix used in this work was a polybutadiene, industrial grade S-200, from Negromex, Inc. Two types of conductive particles were used; carbon-black, type Vulcan XC72, from Cabot Inc., and graphite, type "o" grade 325, from Grafito de Mexico, Inc. The main characteristics of these materials are reported in Tables I–III.

For the present work, a composite was prepared with the following composition; 40% w/w polybutadiene, 25% w/w carbon black, and 35% w/w graphite. The elaboration procedure was as follows: first of all, the materials were dried for 1 h at 105°C. Subsequently, the polybutadiene was dissolved in a nafta from Petroleos Mexicanos, Inc., using a ratio polymer/solvent of 1 : 8 w/w. The graphite and carbon black were added to this solution using a RATIO mixer, model LPM #4, with double vertical blades. The mixing was carried out for 45 min at room temperature and at a speed of 44 rpm. The slurry formed was spread on four trays of 1.2 m^2 and dried for 24 h at 80°C in a chamber with an integrated facility for the extraction and condensation of solvents. Once the solvent was eliminated, the composite was taken from the trays and immediately ground in a Brabender mill, model LS 100L1, and sieved through

a 2-mm mesh. Afterward, it was processed in a laboratory Brabender extruder, model PLE-330, with an L/D ratio of 20. A screw with a compression ratio of 2/1 and a die for filaments of 2 mm in diameter were used to extrude the composite. The process was performed at a temperature of 180°C in the barrel, and 190°C in the die. The screw speed was 20 rpm. A filament of 2.7 ± 0.005 mm in diameter was obtained. This filament was quenched in water, at 25°C, immediately after extrusion. Finally, the filament was wound up. Almost 2000 meters of filament were produced following the previous procedure. To perform the electrical and mechanical tests, samples of 30 cm of this filament were used.

To assess the effect of organic solvents on the electrical properties of the composite, the following solvents were utilised; benzene, diethyl ether, hexane, tetrahydrofurane (THF), and xylene. All these solvents were supplied by Aldrich Inc. Also, two types of gasoline: a leaded one (Nova) and an unleaded one (Magna), supplied by Petroleos Mexicanos, S.A., were used.

Electrical Characterization

The conductivity of the samples was measured at different voltages (0.1–30 V) according to the ASTM B-193 method. These measurements were carried out with a Cole-Palmer multimeter, model 2030–0000, which has a facility to record the current intensity continuously. The samples and the multimeter were connected in series to a BK Dynascan source of direct current, model 1650. Cylindrical copper electrodes of 10 mm length were used to connect the samples to the circuit. Also, to diminish the contact resistance between the electrodes and the specimens they were stuck with silver ink to the extremities of the samples. During the tests, the specimen temperature was continuously monitored using a cromel-alumel thermocouple fixed to its surface. This thermocouple was connected to a Cole-Palmer temperature register, model 8373–72. All the experiments were carried out at room temperature.

Table II Carbon Black Characteristics

Industrial Grade	Vulcan XC72 (Pellets)
Nitrogen surface area (m^2/g)	254
Particle size (nm)	30
Pore volume (dibutyl phthalate absorption, cc/100 g)	178
Pore area (m^2/g)	94
Volatile content (%)	1.500
Density (g/dm^3)	273

Table III Graphite Characteristics

Components	Percent (w/w)
Carbon	96.500
SiO_2	1.610
Fe_2O_3	0.830
H_2O	0.500
Al_2O_3	0.300
Other Impurities	0.260

The variation of the electrical conductivity of the samples, when they come into contact with organic solvents, was evaluated in the following way: a filament specimen was placed at the bottom of a Petri dish of 15 cm in diameter. Its extremities were connected in a similar way as previously described. The electrodes were placed out of the dish. A voltage of 1 V was applied to the filament and the intensity of the current flowing through it was registered continually. Once the steady state was reached, 100 mL of one of the organic solvents was poured into the Petri dish. The voltage was maintained at constant value and the reduction of the current intensity was continuously registered. To evaluate the increase in both length and transverse area of the sample due to swelling, the whole sample and its central part were photographed every 90 s with two Nikkon cameras, model F-601M. One of them, provided with a zoom lens that was focused directly to the central part of the specimen. To calibrate the measures a stainless steel scale was placed at a side of the sample during the tests. Finally, the specimen temperature was monitored in a similar way as previously described.

The preceding procedure was repeated for each solvent, using Petri dishes carefully cleaned and three different filament samples. The variation of material resistivity (ρ) was determined from the current intensity (i) values. This determination was performed taking into account the increase in the transverse section area (a) and length (l) of the filament due to swelling, according to the equation: $\rho = av/li$, where v is the constant voltage applied.

Mechanical Characterization

Five filament samples were submitted to tension at a stretching rate of 10 mm/min in an Instron

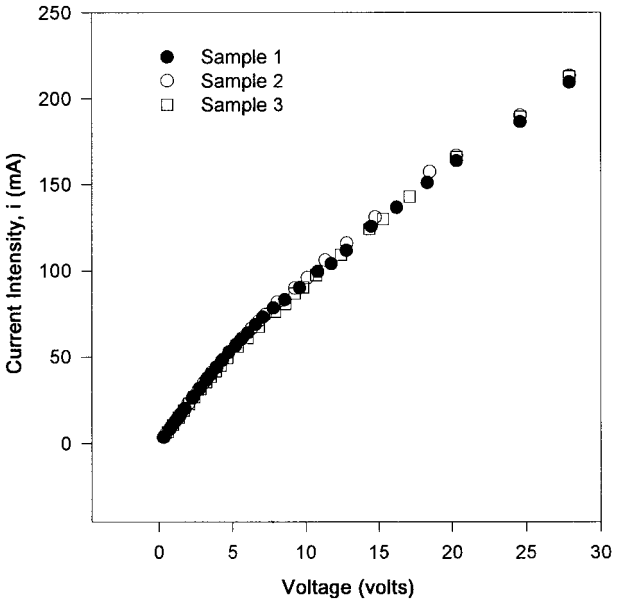

Figure 1 Relation between current intensity and voltage applied.

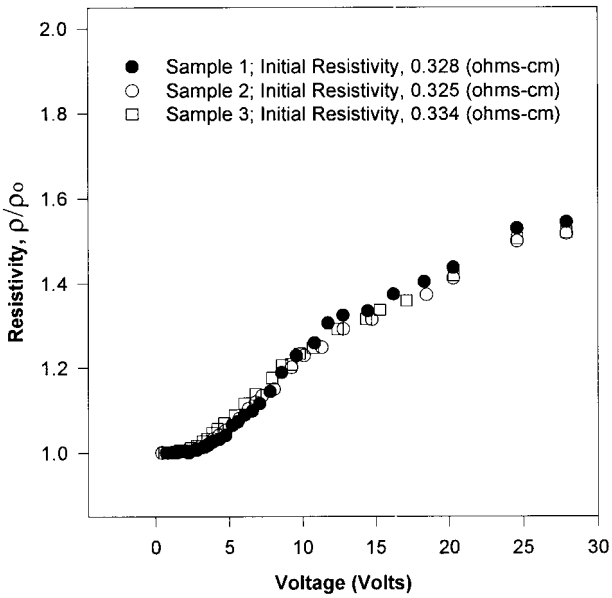

Figure 2 Evolution of the resistivity with the current intensity.

mechanical testing machine, model 1125. Pneumatic clamps were used to hold the specimens. The Young's modulus was measured using a strain gage extensiometer, model 2630–002 according to the ASTM-D638 method. The large strains were evaluated by measuring the distance between two point marks drawn on the samples with an initial separation of 10 mm. The instantaneous distance between the marks was measured by photographic means, according to the method described by G'sell[84] and Uribe.[85]

RESULTS

The measured resistivity of the composite was of 0.33 ± 0.01 Ω cm, at 25 ± 1.0°C (using a voltage of 1.0 V during the measure). This value is in good agreement with the carbon-black supplier standards.[86] It must be mentioned, however, that the resistivity of the polymer composites could vary with the value of the voltage used.[9,87–89] Indeed, Figure 1 shows the relation between the current intensity and the voltage applied. We can observe that at low voltages, less than 5 volts, a linear relationship between the current intensity and voltage is established. The slope in this range corresponds to a resistivity of approximately 0.33 ± 0.01 Ω cm, or to a conductivity of roughly 3.0 Ω^{-1} cm^{-1}. However, at higher voltages another relationship is established corresponding to higher resistivities. The evolution of the resistivity with both current intensity and voltage in the specimens is illustrated in Figures 2 and 3. The composite resistivity stays practically constant up to a voltage of approximately 5 V, corresponding to a current intensity of roughly 50 mA; increasing, however, with higher voltages. This resistivity increase is due to the self-heating of the mate-

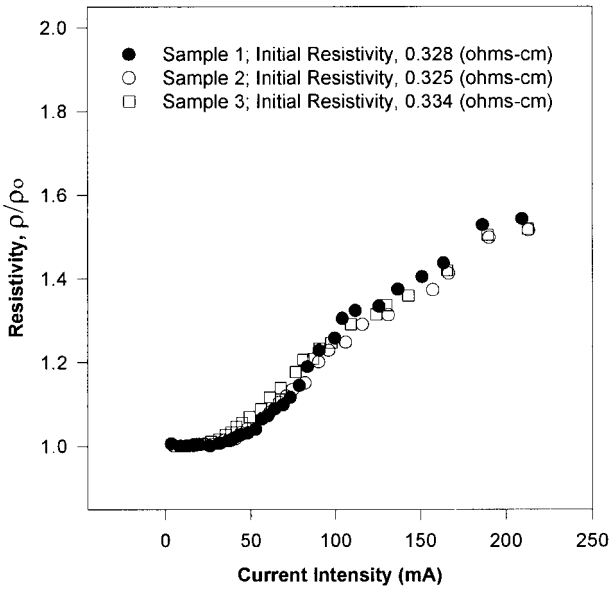

Figure 3 Evolution of the resistivity with the voltage applied.

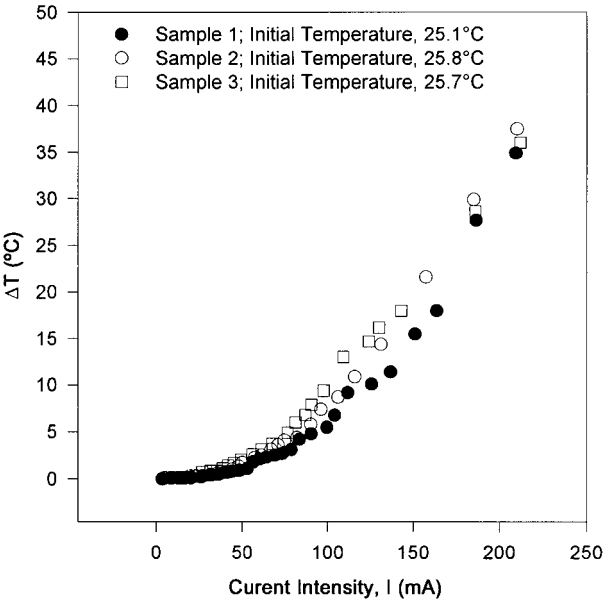

Figure 4 Increase of the resistivity due to self-heating of the material by Joule's effect.

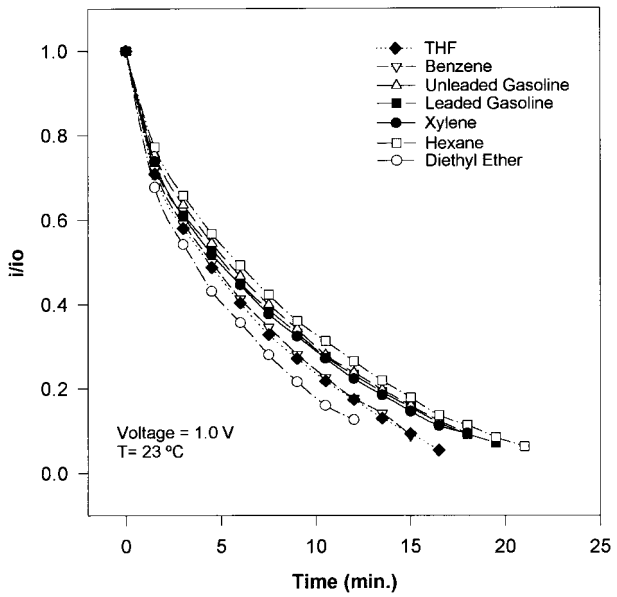

Figure 5 Normalized values of the current intensity through the samples versus the exposure time to solvents.

rial produced by Joule's effect. Indeed, as shown in Figure 4, the self-heating produced by current intensities higher than 50 mA causes a considerable temperature rise, which produces the resistivity increase. Concerning this phenomenon, it must be mentioned that a temperature increase has a dual effect on the resistivity of the carbon–polymer composites. On one hand, a temperature rise favors the electron transport through the polymer layers by tunneling,[79,82,83] because it magnifies the thermal fluctuations. These fluctuations lower the potential barrier established by the polymer between carbon aggregates. This phenomenon promotes the decrease of the composite resistivity[79,83] because the electrons also can be transported through some zones of the matrix and not only through the percolative mats. It must be mentioned, however, that the previous effect is very significant at temperatures close to 0 K, but at higher temperatures it becomes much less important. On the other hand, as the thermal expansion coefficient of the polybutadiene is almost 10 times greater than that of carbon particles,[90,91] a temperature rise produces an increase of the gap width between these particles that hinders the tunnel effect, and even could disconnect some of the particles in the percolative chains, increasing the composite resistivity. It is apparent that these mechanisms have opposing effects; however, at room temperature the effect of the matrix dilation largely surpasses the influence of thermal fluctuations on the composite electrical properties. As a result, at room conditions, a temperature increase causes a net augmentation of the composite resistivity.[83,92,93] Concerning our experiments, we avoid the previous resistivity variation by fixing a voltage of 1 V to perform all the subsequent tests.

Figures 5 and 6 show the normalized values of

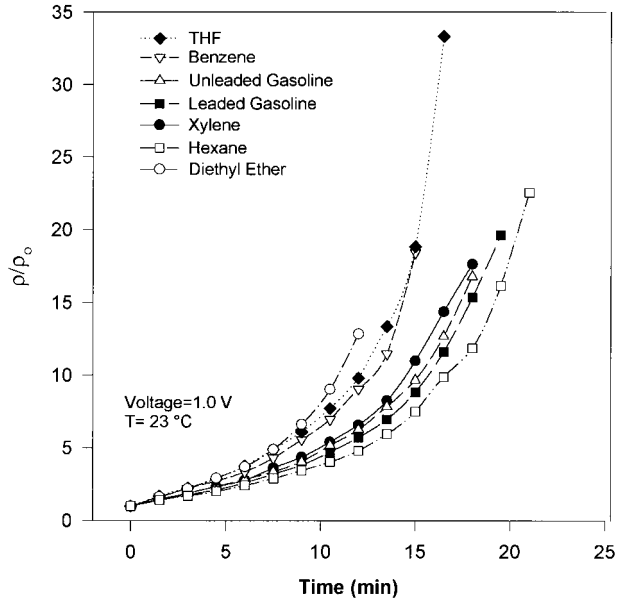

Figure 6 Normalized values of the resistivity of the samples versus the exposure time to solvents.

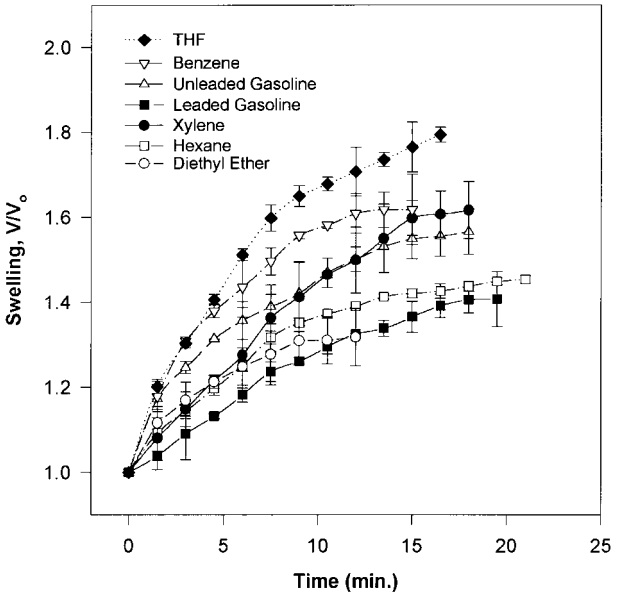

Figure 7 Sample swelling versus the exposure time to solvents.

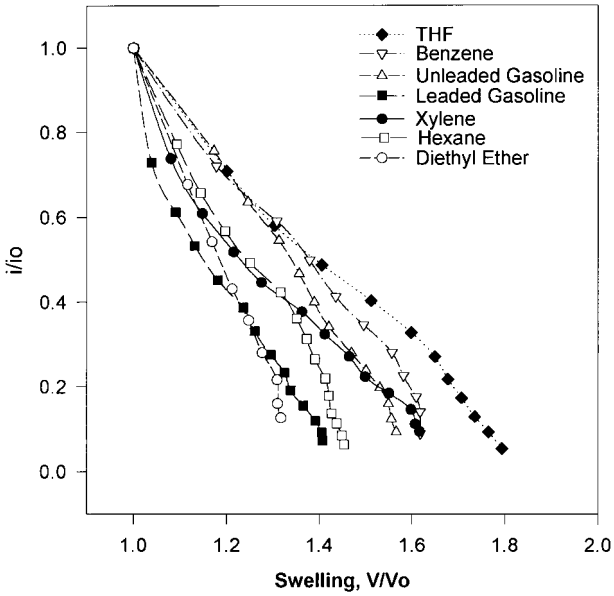

Figure 8 Relation between the current intensity data and sample swelling.

the current intensity (i/i_0) through the samples and their resistivity (ρ/ρ_0) plotted vs. the exposure time of samples to each solvent. It is observed that the current intensity falls while the corresponding resistivity increases with the exposure time. In these figures, each datum represents the average of three different samples (the error bars were not drawn in the figures because they overlap, leading to confusion; however, the experimental error was lower than 5% in all the cases). In these figures it is observed that the diethyl ether produces a faster decrease in current intensity than the other solvents. In contrast, the hexane produces the slowest one. Also, the results show that in contact with solvents the resistivity of the composite increases by roughly 30% after just 1.5 min. More important, the composite conductivity is practically annulled after only 20 min.

Figure 7 shows the rate at which the samples swell when entering in contact with each solvent. In this figure the normalized values of the sample volume (V/V_0) is plotted as a function of the exposure time. It is observed that THF and benzene produce the highest composite swelling, while the leaded gasoline and the diethyl ether caused the lowest one.

Furthermore, Figures 8 and 9 display the relation between the current intensity and the resistivity data in function of the swelling. As expected, the current intensity falls and the resistivity grows when the swelling proceeds. However, in the previous figures, an important influence of the solvent nature on the relationship between the current intensity, or the resistivity, and swelling must be noted. Also, it is interesting to observe that the intensity falls and the resistivity grows in a monotonical way until an approximately normalized intensity i/i_0 of 0.35, or a normalized resistivity ρ/ρ_0 of 5, when a very defined inflection

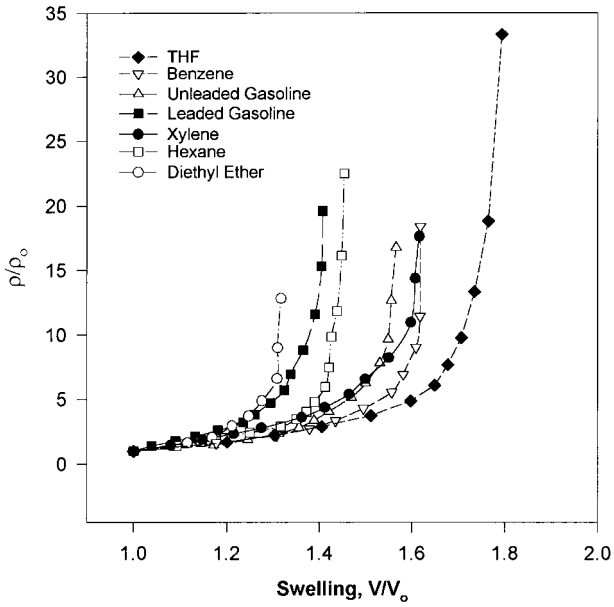

Figure 9 Relation between the resistivity values and sample swelling.

point appears. This point indicates a change in the electron transport mechanisms inside the composite. This change is mainly due to the drastic diminution of the particle volume fraction into the composite (due to the introduction of the solvent) that becomes closer to the percolation threshold.[87] Or, in other words, it is due to the separation of the particle clusters by the solvent, thus disconnecting the percolation networks. It is important, however, to mention that the previous change could be enhanced by the appearance of flaws in the material, produced by the matrix swelling, that could block the electrical flow. For example, it was observed that the diethyl ether promotes the formation of fissures in the composite when the matrix swells. This phenomenon prevents the current flow in the filament, producing a faster diminution of the current intensity and the subsequent decrease of the overall composite conductivity.

Finally, the results of the mechanical characterisation show that the samples had an average Young's modulus of 124 ± 3.5 MPa, an average maximum strength of 15.5 ± 0.05 MPa, and an average strain at break of 0.265 ± 0.015 (see Table IV). These results indicate that the material resistance and flexibility are definitely enough to permit the handling of the filament and the use of it as a sensor in any standard chemical installation.

ANALYSIS AND DISCUSSION

As previously mentioned, in the present work we use the generalized effective media (GEM) equation proposed by McLachlang[8] to model the influence of swelling on the composite resistivity. This equation relates the medium resistivity to the resistivities and volume fractions of its components by the following expression:

$$\frac{f(\rho_H^{-1/t} - \rho_M^{-1/t})}{\rho_H^{-1/t} + f_R\rho_H^{-1/t}} + \frac{(1-f)(\rho_L^{-1/t} - \rho_M^{-1/t})}{\rho_L^{-1/t} + f_R\rho_M^{-1/t}} = 0 \quad (1)$$

$$f_R = \frac{f_C}{1-f} \quad (2)$$

where ρ_L, ρ_H, and ρ_M are the resistivities of low and high resistivity components and the composite itself, respectively. As well as, f and f_C are the volume fraction and the critical volume fraction of the high resistivity component. f_R is defined by eq. (2), and t is an exponent related to a combination of effective demagnetisation coefficients and the critical volume fraction f_C.

The previous equation could be solved for ρ_M, giving the next expression:

$$\rho_M = \left\{ -\frac{1}{2f_C}\left((\alpha-\beta)f + \beta - \sqrt{\gamma f^2 + \delta f + \varepsilon}\right)\right\}^{-t} \quad (3)$$

where

$$\alpha = \rho_L^{-1/t} - \rho_H^{-1/t} f_R \quad (4)$$

$$\beta = \rho_H^{-1/t} - \rho_L^{-1/t} f_R \quad (5)$$

$$\gamma = \rho_L^{-1/t}(\rho_L^{-1/t} - 2\rho_H^{-1/t})(f_R + 1)^2 \quad (6)$$

$$\delta = 2\rho_L^{-1/t}(f_R + 1)(\rho_H^{-1/t} f_R + \beta) \quad (7)$$

$$\varepsilon = \rho_L^{-1/t} f_R(\rho_L^{-1/t} f_R + 2\rho_H^{-1/t}). \quad (8)$$

This equation is valid for a system of only two components. However, we can utilize it if the following approximations are accepted: (1) As the resistivities of polymer matrix and solvents are of the same order of magnitude, and they are substantially different from the resistivity of the carbon particles, we may treat both phases (polymer and solvent) as a unique phase. Then, using the swelling data, it is possible to evaluate the instantaneous value of the high resistivity volume fraction f. (2) Also, we may impose to this phase an arbitrary high resistivity value ($\rho_H = 1 \times 10^{16}$ Ω cm), which is in the order of magnitude of the real values. This last assumption can be made, because if we use, in the interval studied, the value of the polymer resistivity or that of the solvent to evaluate the result of expression (1), the resulting composite conductivity differs in less than a 10^{-15}%. (3) Similarly, we have utilized as the low resistivity value ρ_L, the value that predicts correctly the experimental resistivity of the composite evaluated. This value was of $\rho_L = 8 \times 10^{-2}$ Ω cm. It is important to observe that the last value is almost equal to the graphite resistivity ($\rho_L = 8.7 \cdot 10^{-2}$ Ω cm).

Using the previous approximations, the GEM equation was fitted to the experimental data. Figure 10 shows the theoretical prediction of the previous equation (continuous lines). We can observe that this model predicts very satisfactorily the experimental results (points).

In Table V the values of f_C and t, for each sol-

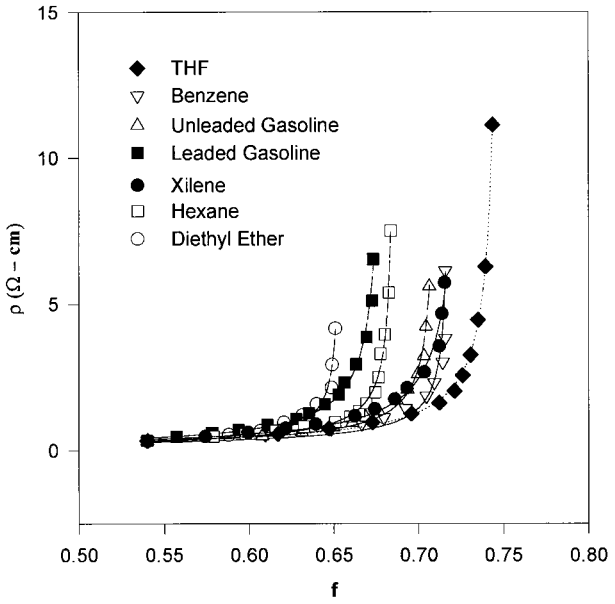

Figure 10 Comparison between the experimental resistivity values and the theoretical ones.

vent are reported. The first parameter, f_C, varies between 0.65 and 0.75, while the second one, t, varies between 0.68 and 0.98. These values are similar to the equivalent parameters previously calculated in the literature.[8] However, it is important to observe the influence of the solvent nature on the value of these parameters. This question could have several answers. First of all, the solvents utilized have different molecular sizes and diffusion coefficients. Therefore, its concentration profiles through the transverse section of the filament must be unequal, producing a distinct swelling behavior in the bulk rather than on the skin of the filaments. It is also possible that solvents would be heterogeneously distributed in the composite. Indeed, some solvents could be exclusively concentrated in the matrix, while others could be located in the matrix and in the interface between the particle clusters and matrix, or even at the interior of the clusters. To have an idea of the importance of the previous factors, the diffusion coefficient of solvents in the composite has been evaluated following the method described by Crank.[77] The solvent molecular weight was obtained from tables,[101] and a wetting coefficient defined by eq. (9) has been evaluated.

$$\omega_{\text{polymer-carbon}} = (\gamma_{\text{solvent-carbon}} - \gamma_{\text{solvent-polymer}})/\gamma_{\text{polymer-carbon}} \quad (9)$$

where γ_{i-j} is the interfacial free energy of the i–j interfase. This coefficient is a measure of the affinity of a substance to each phase of a composite.[34,100] By using this last parameter and similar arguments other than Miyasaka,[34,100] the next phenomenon could be predicted:

when

$\omega_{\text{polymer-carbon}} > 1$ the solvent distributes within the polymer phase

$-1 < \omega_{\text{polymer-carbon}} > 1$ the solvent distributes at the interface

$\omega_{\text{polymer-carbon}} < -1$ the solvent distributes in the carbon clusters.

The values obtained for the diffusion coefficient, the molecular weight, and the wetting coefficient are listed in Table VI.

Furthermore, in Figures 11–13 the influence of the previous parameters on the critical volume fraction f_c and the exponent t is shown. The two first parameters (diffusion coefficient and molecular weight) do not have apparent influence on the values of f_c and t. In contrast, the wetting coefficient seems to have a definitive influence on these values. It is apparent that when this coefficient approaches -1, the corresponding values of f_c and t increase.

It is interesting also to note that, even though all the $\omega_{\text{polymer-carbon}}$ values are inferior to -1, when it approaches -1, there is a possibility that a solvent fraction would be placed at the interface between carbon clusters and matrix instead of just in the matrix. It is important to note that, in our experiments, a high value of f_c means that an additional volume of absorbed solvent is necessary to reach the percolation threshold (see Fig. 10). Then, it seems reasonable to consider that the solvent fraction placed at the interface exerts a smaller influence on the resistivity increase than the solvent fraction concentrated in the matrix. This could be explained by considering that the solvent in the interface exerts a pressure on the percolation chains but do not separate them. In contrast, the solvent concentrated exclusively in the matrix separates these chains in a more effec-

Table IV Mechanical Properties of the Composite

Young modulus (MPa)	123.98 ± 3.50
Maximum strength (MPa)	15.5 ± 0.05
Strain at break (%)	30.0 ± 2.0

Table V f_c, ϕ_c, and t Values Obtained from the Fit of the McLachlang Equation to the ρ Versus f Curves

Solvent	f_c	ϕ_c	t
THF	0.748	0.252	0.938
Hexane	0.686	0.314	0.762
Benzene	0.723	0.277	0.851
Xylene	0.728	0.272	0.982
Diethyl ether	0.654	0.346	0.687
Leaded gasoline	0.681	0.319	0.919
Unleaded gasoline	0.711	0.673	0.807

tive way. On the other hand, as previously mentioned, some solvents (as, e.g., the diethyl ether) promotes the formation of fissures in the matrix leading to a disconnection of several sections of the filament. Then this phenomenon could diminish the volume fraction of solvent needed to reach the percolation threshold. However, it is evidently necessary to perform a more detailed study to elucidate the previous behavior.

Finally, it is important to stress that the composite obtained is a very promising material that can be utilized in several applications. For example, the composite filaments can be integrated in a convenient casing into a leak detection system, which can monitor the periphery of reservoirs and containers that stocks gasolines and organic solvents,[4] considering that a fall of 10% in the current intensity is a convenient threshold to set off an alarm system when a leak is produced.[1–4] We can see that these filaments, conveniently disposed on the pipes and containers, need only about 36 s to detect the leak. Therefore, a system based on the use of this material can be very sensitive and efficient.

CONCLUSIONS

A conductive composite was obtained by mixing a polybutadiene rubber with carbon black and graphite particles, in a specific proportion, through a mixing process in solution followed by the extrusion of the material. The conductivity of the composite obtained, in the form of filaments, was 3.0 ± 0.1 (Ω^{-1} cm^{-1}). It has been observed, however, that this conductivity depends on the voltage applied. This variation is not significant for voltages that produce current intensities lower than 50 mA; nevertheless, when higher intensities are produced the conductivity falls as much as 30%. This fall is due to the increase in temperature produced by Joule's effect. Indeed, this temperature increase is small at current intensities lower than 50 mA.

Moreover, the swelling test performed with several organic solvents shows that the electrical resistivity of the composite increases very fast with the exposure time, observing a reduction of 30% of the initial conductivity after 1.5 min, and of 60% after 5 min, of exposure to these solvents. To model the previous behavior, an effective media percolation approach was used. This approach was adapted to the needs of our experiments by modifying the definition of one of its main parameters (the critical volume value of the nonconductive fraction). The experimental data were successfully described by this model. Also, we found that the effect of swelling on the composite conducting capacity depends notably on the solvent

Table VI Values of the Diffusion Coefficient, Molecular Weight, and Wetting Coefficient Used

Solvent	Diffution Coefficient $\times 10^6$ (cm^2 s^{-1})	Molecular Weight (mol/g)	$\omega_{\text{Polymer-carbon}}$
THF	3.799	72.000	−1.520
Hexane	2.841	86.000	−2.460
Benzene	2.671	78.000	−1.260
Xylene	2.673	93.000	−1.320
Diethyl ether	3.571	74.000	−2.650

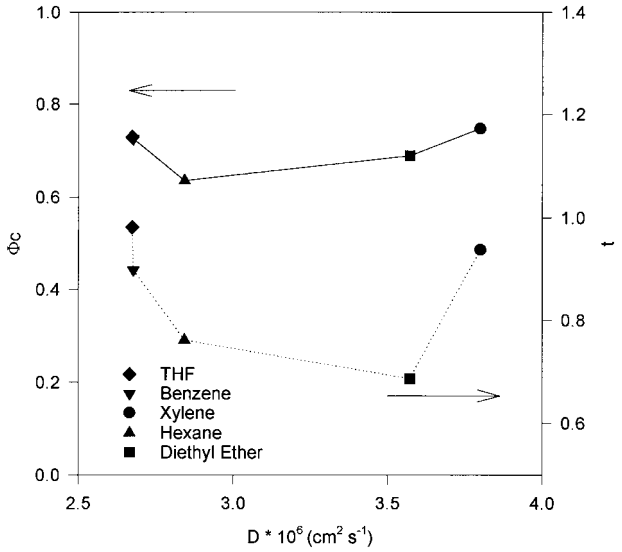

Figure 11 Influence on the solvent diffusion coefficient into the samples on the critical volume fraction and the exponent t values.

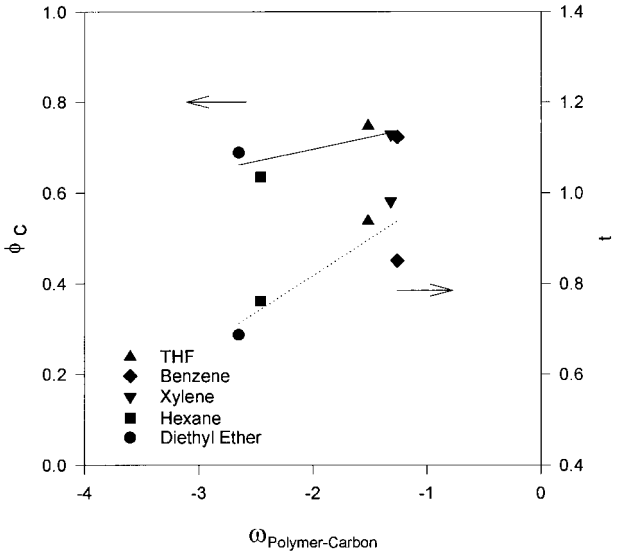

Figure 13 Influence on the wetting coefficient on the critical volume fraction and the exponent t values.

nature. This behavior could be attributed mainly to the distinct distribution of solvents into the composite phases and interfaces, another possible origin of this dependence is the tendency of some solvents to promote the formation of fissures in the matrix leading to disconnection of some sections of the filament.

Finally, it is important to stress that this composite is relatively flexible and mechanically resistant, being very easy to handle and prepare.

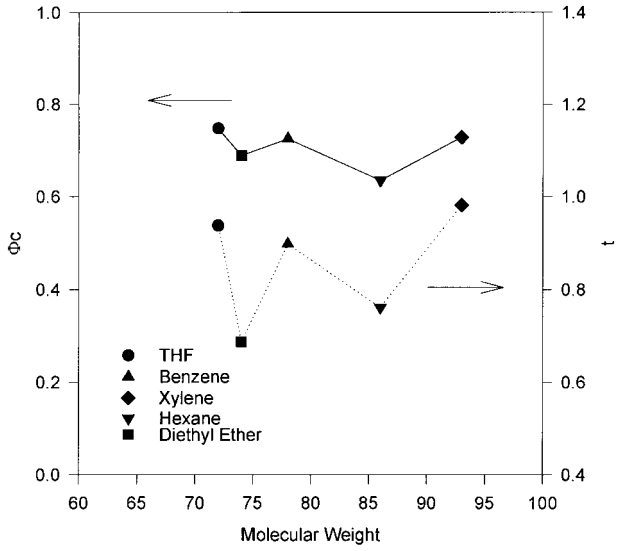

Figure 12 Influence of the solvent molecular weight of the samples on the critical volume fraction and the exponent t values.

The authors are grateful to CONACyT for the award of the Research Grant No. G500–551/95, to Jafet Quijano for his assistance in performing several of the mathematic calculations, and to Ingrid Olmsted for her useful advice.

REFERENCES

1. M. C. Lonergan, E. J. Severin, B. J. Doleman, S. A. Beaber, R. H. Grubbs, and N. S. Lewis, *Chem. Mater.,* **8,** 2298 (1996).
2. B. Lundberg and B. Sundqvist, *J. Appl. Phys.,* **60,** 1074 (1986).
3. T. Kudo, U.S. Pat. No. 5,378,995 (1995).
4. Y. Ijiri, T. Kudo, and Y. Shiraiwa, US Pat. No. 1,173,684 (1992).
5. J. Akiba, U.S. Pat. No. 4,896,527 (1990).
6. A. Marquez, U.S. Pat. No. 5, 288,458 (1994).
7. K. Sherman, L. Middenman, and S. Jacobs, *Polym. Eng. Sci.,* **23,** 36 (1983).
8. M. Blaszkiewcz, D. McLachlang, and R. E. Newnham, *Polym. Eng. Sci.,* **32,** 421 (1992).
9. F. Lux, *Polym. Eng. Sci.,* **33,** 334 (1993).
10. R. Zalllen, in *The Physics of Amorphous Solids,* Wiley, New York, 1983, and references therein.
11. S. Kirpatrick, *Rev. Mod. Phys.,* **45,** 574 (1973).
12. J. Jansen, *J. Appl. Phys.,* **46,** 966 (1975).
13. G. E. Pike and C. H. Seager, *Phys. Rev.,* **10,** 1421 (1974).
14. G. E. Pike and C. H. Seager, *Phys. Rev.,* **B10,** 1435 (1974).
15. F. S. Clarke, J. W. Orton, and J. Guest, *Phys. Rev.,* **18,** 1814 (1978).

16. X. Quan, *J. Polym. Sci. B, Polym. Phys.,* **25,** 1557 (1987).
17. S. Etemand, X. Quan, and N. A. Sanders, *Appl. Phys. Lett.,* **48,** 607 (1986).
18. J. I. Yamaki, O. Maeda, and Y. Kayayama, *Rev. Elec. Commun. Lab.,* **26,** 616 (1978).
19. S. M. Aharoni, *J. Appl. Phys.,* **43,** 2463 (1972).
20. J. Gurland, *Trans. Met, Soc. AIME,* **236,** 642 (1966).
21. R. M. Scasbrick, *J. Phys. D Appl. Phys.,* **6,** 2098 (1973).
22. F. Buech, *J. Appl. Phys.,* **43,** 4837 (1972).
23. T. A. Ezqierra, M. Kulescza, C. Santa Cruz, and F. J. Balta Calleja, *Adv. Mater.,* **2,** 597 (1990).
24. L. Benguigui, J. Yacubowicz, and M. Narkis, *J. Polym. Sci. B, Polym. Phys.,* **25,** 127 (1987).
25. S. Reich, *J. Mater. Sci.,* **22,** 3391 (1987).
26. J. Yacubowicz and M. Narkis, *Polym. Eng. Sci.,* **26,** 1568 (1986).
27. A. Andreatta, S. Tokito, P. Smith, and A. J. Heeger, *Mol. Cryst. Liq. Cryst.,* **189,** 169 (1990).
28. A. Andreatta, A. J. Heeger, and P. Smith, *Polym. Commun.,* **31,** 275 (1990).
29. S. Hotta, S. D. D. V. Rughooputh, and A. J. Heeger, *Synth. Met.,* **22,** 79 (1987).
30. M. Aldissi, *Synth. Met.,* **13,** 87 (1986).
31. M. Sumita, K. Sakata, S. Asai, K. Miyasaka, and H. Nakagawa, *Polym. Bull.,* **25,** 265 (1991).
32. M. Sumita, S. Asai, K. Miyadera, E. Jojima, and K. Miyasaka, *Coll. Polym. Sci.,* **264,** 212 (1986).
33. M. Sumita, H. Abe, H. Kayaki, and K. Miyasaka, *J. Macromol. Sci. Phys.,* **B25,** 171 (1986).
34. K. Miyasaka, K. Watanabe, E. Jojima, H. Aida, M. Sumita, and K. Ishikawa, *J. Mater. Sci.,* **17,** 1610 (1982).
35. B. Wessling, *Synth. Met.,* **28,** C849 (1989).
36. B. Wessling, H. Volk, W. R. Mathew, and V. G. Kulkarni, *Mol. Cryst. Liq. Cryst.,* **160,** 205 (1988).
37. B. Wessling, *Synth. Met.,* **27**, A83 (1988).
38. B. Wessling, G.B. Pat. 8901424.5 (1988).
39. B. Wessling and H. Volk, *Synth. Met.,* **18,** 671 (1987).
40. B. Wessling, *Makromol. Chem,* **185,** 1265 (1984).
41. B. Wessling and H. Voke, *Synth. Met.,* **15,** 183 (1986).
42. B. Wessling, in *Electronic Properties of Polymers,* Springer-Verlag, Heidelberg, 1988, p. 407.
43. B. Wessling, *Kunststoffe,* **80,** 323 (1990).
44. S. Radhakrishnan, *Polym. Commun.,* **26,** 153 (1985).
45. T. Slupkowski, *Phys. Status Solids,* **A83,** 329 (1984).
46. C. Rajagopal and M. Satyam, *J. Appl. Phys.,* **49,** 5536 (1978).
47. A. Malliaris and D. T. Turner, *J. Appl. Phys.,* **42,** 614 (1971).
48. S. K. Bhattacharya and A. C. D. Chaklader, *Polym. Plast. Technol. Eng.,* **19,** 21 (1982).
49. K. Yoshida, *J. Phys. Soc. Jpn.,* **59,** 4087 (1990).
50. F. M. Fowkes, *Ind. Eng. Chem.,* **56,** 40 (1964).
51. R. L. McCullough, *Comp. Sci. Technol.,* **22,** 3 (1985).
52. M. A. Berger and R. L. McCullough, *Comp. Sci. Technol.,* **22,** 81 (1985).
53. B. Schulz, *High Temp. High Press.,* **13,** 649 (1981).
54. G. Ondracek, *Metall.,* **36,** 523 (1982).
55. G. Ondracek, *Metall.,* **36,** 1288 (1982).
56. G. Ondracek, *Metall.,* **37,** 1016 (1983).
57. I. E. Nielsen, *Ind. Engng. Chem. Fund.,* **13,** 17 (1974).
58. S. Ahmed and F. R. Jones, *J. Mater. Sci.,* **25,** 4933 (1990).
59. S. Tokito, P. Smith, and J. Heeger, *Synth. Met.,* **36,** 183 (1990).
60. D. M. Bigg, *J. Rheol.,* **28,** 501 (1984).
61. J. R. Harbour and M. J. Walzak, *J. Colloid Interface Sci.,* **119,** 150 (1987).
62. K. H. Möbius, *Kunststoffe,* **78,** 53 (1988).
63. J. M. Machado, F. E. Karasz, and R. W. Lenz, *Polymer,* **29,** 1412 (1988).
64. T. A. Ezquerra, R. K. Bayer, and F. J. Balta Calleja, *J. Mater. Sci.,* **23,** 4121 (1990).
65. K. A. Mazich, M. A. Samus, P. C. Killgoar, Jr., and H. K. Plummer, *J. Rubber Chem. Tehcnol.,* **59,** 623 (1986).
66. M. Y. Boluk and H. P. Schreiber, *Polym. Compos.,* **10,** 215 (1989).
67. A. Vidal and J. B. Donnet, *Prog. Colloid Polym. Sci.,* **75,** 201 (1987).
68. T. A. Ezquerra, R. K. Bayer, and F. J. Balta Calleja, *Prog. Colloid Polym. Sci.,* **23,** 4121 (1988).
69. J. Martinez Salazar, R. K. Bayer, T. A. Ezquerra1, and F. J. Balta Calleja, *Colloid Polym. Sci.,* **267,** 409 (1989).
70. M. E. Galvin and G. E. Wnek, *J. Polym. Sci., Chem. Ed.,* **21,** 2727 (1983).
71. L. Watanabe, K. Hong, and F. Rubner, *Langumir,* **6,** 1164 (1990).
72. B. D. Malhorta, S. Gosh, and R. Chandra, *J. Appl. Polym. Sci.,* **40,** 1049 (1990).
73. J. R. Harbour, M. J. Walzak, and R. P. Veregin, *J. Colloid Interface Sci.,* **138,** 380 (1990).
74. L. Nicodemo, L. Nicolais, and E. Scafora, *Polym. Eng. Sci. Len.,* **18,** 293 (1978).
75. T. Noguchi, K. Gotoh, Y. Yamaguchi, and S. Deki, *J. Mater. Sci. Len.,* **10,** 477 (1991).
76. G. Geuskens, E. Dekezel, S. Blacher, and F. Brouers, *Eur. Polym. J.,* **27,** 1261 (1991).
77. J. Crank, in *The Mathematics of Diffusion,* Oxford Science Publications, Uxbrigde, 1986.
78. K. L. Tan, B. T. G. Tan, S. H. Khor, K. G. Neoh, and E. T. Kang, *J. Phys. Chem. Solids,* **52,** 673 (1991).

79. K. Sichel and G. Sheng, in *Carbon Black-Polymer Composites,* Marcel Dekker Inc., New York, 1993.
80. J. Simmons, *J. Appl. Phys.,* **34,** 1793 (1963).
81. P. Sheng, E. K. Sichel, and J. I. Gittleman, *Phys. Rev. Lett.,* **40,** 1197 (1978).
82. E. K. Sichel, J. I. Gittleman, and P. Sheng, *Phys. Rev.,* **B18,** 5712 (1978).
83. A. Medalia, *Rubber Chem. Technol.,* **59,** 432 (1985).
84. C. G'sell and A. Marquez-Lucero, *Polymer,* **34,** 2740 (1993).
85. J. Uribe, Chemical Engineering Thesis, Facultad de Ingeniería Química, Universidad Autónoma de Yucatán (1995).
86. D. J. Sommers, *Tecnical Report S-39,* Cabot Corporation, 125 High Street, Massachusetts 02120, 1994.
87. F. Lux, *J. Mater. Sci.,* **28,** 285 (1993).
88. A. Abo-hashem, *J. Appl. Polym. Sci.,* **45,** 1733 (1992).
89. M. Narkis, A. Ram, and Z. Stein, *Polym. Eng. Sci.,* **21,** 1049 (1981).
90. Y. S. Touloukian, Ed., in *Thermal Expansion-Non-Metallic Solids, Thermophysical Properties of Matter,* vol. 13, Plenum Press, New York, 1977.
91. H. Barth, *Mod. Plast. Encycl.,* **53,** 10A (1976).
92. H. Tang, Z. Y. Liu, J. H. Piao, X. F. Chen, Y. X. Liu, and S. H. Li, *J. Appl. Polym. Sci.,* **51,** 1159 (1994).
93. P. Bengtsson, J. Kubát, C. Klason, and D. McQueen, *Polym. Eng. Sci.,* **33,** 573 (1993).
94. P. Beadle and S. Armes, *Macromolecules,* **25,** 2526 (1992).
95. B. Tieke and W. Gabriel, *Polymer,* **31,** 20 (1990).
96. B. Lee, *Polym. Eng. Sci.,* **32,** 36 (1992).
97. R. Crossman, *Polym. Eng. Sci.,* **25,** 507 (1985).
98. A. Sarkan, *Polym. Eng. Sci.,* **32,** 305 (1992).
99. I. Chmutin, S. Letyagin, and A. Ponomarenko, *Polym. Sci.,* **36,** 576 (1994).
100. S. Asai. K. Sakata, M. Sumita, and K. Miyasaka, *Polym. J.,* **24,** 415 (1992).
101. A. Braton, *CRC Handbook of Solubility Parameters and other Cohesion Parameters,* CRC Pres Inc., Boca Raton, FL, 1983.